THESIS FOR THE DEGREE OF LICENTIATE OF ENGINEERING

Flow structures in solid-liquid suspensions in mixing and confined jets

MATTHIAS ENG

Chemical Engineering
Department of Chemical and Biological Engineering
CHALMERS UNIVERSITY OF TECHNOLOGY

April 2012

Flow structures in solid-liquid suspensions in mixing and confined jets
MATTHIAS ENG

Licentiatuppsatser vid Institutionen för kemi- och bioteknik Chalmers tekniska högskola
Serie Nr 2012:7
ISSN 1652-943X

Department of Chemical and Biological Engineering
Chalmers University of Technology
SE-412 96 Göteborg, Sweden

Chalmers Reproservice
Göteborg, Sweden 2012

Flow structures in solid-liquid suspensions in mixing and confined jets

Matthias Eng
Chemical Engineering
Department of Chemical and Biological Engineering
Chalmers University of Technology
SE-412 96 Göteborg, Sweden

Abstract

This thesis investigates the influence of solid particles on different liquid flow systems. Large-scale periodic fluctuations such as macro instability (MI) phenomena in a mixing vessel and jet flows in a confined jet were experimentally analyzed by means of LDV. The influences of different sized (0.5mm-2mm) glass particles (0%vol - 6.2%vol) on the velocity and turbulence distribution in a jet were investigated, as well as the effects of varying the amounts of solid particles (up to 11.8%vol) on the frequency and amplitude of macro instabilities. Two component LDV measurements were conducted at different locations in the jet and in the mixing vessel. The values were evaluated using the Lomb algorithm to obtain frequency spectra of the liquid flow. The average axial and lateral velocities, as well as RMS distributions, were determined together with the integral length scale in the confined jet to analyse particle effect. The particle Stoke number was evaluated for the different sized particles and the different flow situations.

The results showed that the MI frequency is not influenced by the addition of solids. However, the MI amplitude was reduced by the addition of the solid phase although still detectable up to the highest concentration measured (11.8 %vol). The particles (1.5mm) with a Stokes number of 1.1, related to the time scale of MI phenomena, caused an increase in MI strength at intermediate solids loading. This phenomenon could not be observed for smaller particles.

No change in the rate of decrease of the centreline velocity or the jet expansion ratio could be observed in the confined jet configuration. The RMS values in the jet increased at high particle loadings; the increase was particularly pronounced in the shear layer close to the nozzle. With increasing particle size a greater effect on the RMS values could be observed. The frequency spectra of the flow and the strength of the large-scale instabilities were only affected by the suspension with the 2mm particles. The 2mm particles had a stabilizing effect on the jet and moved the instability further downstream while the frequency was unaffected.

Acknowledgments

I would like to thank everyone who has helped me in my work in the most recent years and made it possible for this thesis to be written.
First I would like to thank Professor Anders Rasmuson for giving me the opportunity to do my PhD at Chalmers. And that as my supervisor he was always available and spent time and energy to giving me advice and putting me back on track.

For the technical help in building and repairing my equipment I would like to thank Lars-Göran Johanneson and Jan Emnér. Gunnar Johannson is gratefully acknowledged for helping me out with the LDV and for loaning me his equipment.

Special thanks to my close colleagues to share work and spare time. To Per who, as my roommate, had to listen all day long to stories I was telling. And thanks to all my other colleagues and former colleagues who helped me and supported my project.

Finally I want to thank my girlfriend Maria for supporting and encouraging me when I was complaining about the lack of progress in my work.

List of Publications

The work of this thesis is based on the following pubilcations:

- **Influence of solids on macro-instabilities in a stirred tank**
  Matthias Eng and Anders Rasmuson
  Chemical Engineering Research and Design
  In print

- **Measurement of continuous phase velocities in a solid-liquid jet using LDV**
  Matthias Eng and Anders Rasmuson
  Submitted

Contents

1

Introduction

1.1 Background

In most chemical processes multi-phase fluids play a major role. Whether this is the droplet flow in a spray, the mixing of two liquids or the fluidization of solid fuel particles, the interaction between the phases will affect flow structures. While the flow of a single gaseous or a single liquid phase might be well understood for most flow situations, the description of multiphase conditions lacks information. To better understand turbulences, shear forces and the momentum transfer in a fluid under the influence of a secondary phase more detailed investigations are needed.

Numerical simulations in the field of multi-phase systems improve continuously, but the tools are still limited to special cases. Models lack general validity especially for solid particles in the dispersed phase. Model assumptions and simplifications make it impossible to predict the influence of different sized particles on a continuous fluid. There are studies which model every particle separately in a flow, but due to computational demands they are limited to small and idealized systems.

Experimental investigations of multi-phase systems can deliver reliable data to observe and understand mechanisms in suspensions; at the same time they can give information well needed to improve and optimize numerical models. Laser-based optical measurement techniques are non-invasive and can investigate flow situations like bubble flow, droplet sprays and particle suspensions.

Stirred tanks are widely used in the chemical process industry. Mean flows using standard configurations are generally accepted to be well understood. Instantaneous flow, on the other hand, is extremely complex; it varies due to predictable mechanics like axis rotation and the passage of the blade of the impeller, and unpredictable high frequency phenomena, turbulence and low frequency quasi-stationary phenomena. These low frequency phenomena are usually referred to as macro instabilities (MI) and affect the flow pattern which in turn affects large-scale mixing.

Jet flows are one of the most common flow configurations. They occur directly as injection jet sprays or indirectly as part of more complex flow configurations such as fluidized beds, or the discharge of radial and axial mixing impellers. Jets are characterized by a large velocity gradient between two fluids which builds up a shear layer. With increasing distance from the nozzle jets can become unstable and large-scale vortices with a low frequency dominate the flow under this condition. This thesis and the presented studies focus on the influence of solid particles on the flow properties of a liquid carrier phase. Solid particles in a liquid flow are a common but not very detailed investigated configuration in process industry. Having more knowledge about the turbulence structures, the velocity distribution and the mixing behaviour of solid particles in liquid flows can help make these processes more efficient, improve equipment and optimize the prevention of mechanical damage.

1.2 Objectives

The objective of this thesis is to investigate how flow structures in a mixing vessel and in a liquid jet are influenced by the presence of solid particles. Suspensions with increasing particle concentrations were experimentally observed. Particles with different sizes were investigated to capture size dependencies on the solid-phase effect. Special interest is on turbulence variation and the influence of particles on large-scale instabilities. It is often mentioned that MI phenomena could cause an increase in the off-bottom suspension of solids and improve mixing due to their capability to break up the clear fluid layer which forms near the top of a stirred multi-phase tank.

Variations in the turbulence of the shear layer and the large vortices would significantly influence the momentum transport in a jet. Large-scale jet instabilities play a major role in the distribution of solid particles from the jet centre into the fluid bulk.
A two-component LDV was used to obtain velocity data on the liquid flow. Post-processing of the data gave average velocities and RMS profiles. Frequency analysis of the flow and interpretation of the integral length scales were conducted to obtain further insight into the larger instabilities of the suspensions in the mixing vessel and in the jet.

1.3 Outline of the thesis

Chapter 2 gives an overview of the theoretical background of the thesis. The basics of particle flow are presented together with additional knowledge about the flow applications studied. Flow properties in mixing vessels and the structures in a fluid jet are described. Chapter 3 explains the experimental setup used for this thesis. The flow equipment and the measurement technique used for the experiments are presented. The post-processing of the obtained data and the experimental procedure are described as well. Some example results of the studies are shown in Chapter 4 and the conclusions from the investigations are presented in Chapter 5. The two papers are attached last.

2

Theory

2.1 Fluid dynamics of particles

Depending on particle concentration, particle momentum and the flow structures of the carrier phase, different phenomena can dominate the description of particle flow (Crowe et al. [1]). A flowing fluid applies forces on a particle in a suspension. Due to these forces which make the particle flow in a fluid the particle will change direction and velocity. The extent to how much flow can influence particle movement is dependent on the ratio between particle inertia and drag. A particle with a low mass will more easily follow a fluid flow than a high density particle. The particle Stokes number is an important measure of fluid-particle interaction. The Stokes number describes the ratio between the particle relaxation time and a characteristic time scale of the flow (equ.2.1).

$$Stokes = \frac{\tau_p}{\tau_i} \tag{2.1}$$

$$\tau_p = \frac{\rho_p d^2}{18\mu_l} \tag{2.2}$$

The particle relaxation time (equ.2.2) is a measure of the ability of the particle to be influenced by the flow, which, as mentioned, can be described as a relation between particle inertia and drag. The characteristic time scale of the flow relates to a certain fluctuation or change in direction of the flow.

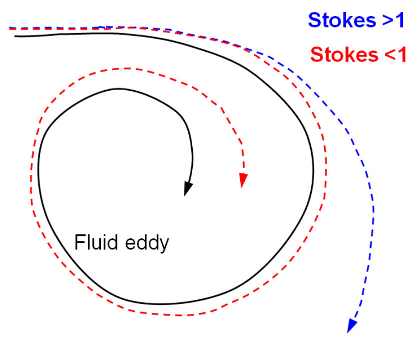

Figure 2.1: Trajectories of particles with different Stokes number

If the Stokes number of a particle is significantly larger than one, the particle trajectory will barely be influenced by a flow structure with this time scale (fig.2.1). For a Stokes number considerably smaller than one, it can be assumed that the particle will follow the fluid to a very large extent. If the Stokes number is equal to one, then the fluid and the particle will have the same time scale and will influence each other.

A fluid will be influenced as well by the presence of particles. A fluid and particles are in a permanent state of exchange of momentum. Due to their inertia particles can slow down a decrease in fluid velocity, but will also take kinetic energy from the fluid when accelerating. This interaction is not completely clear yet when particles are confronted with fluid turbulence. Particles can cause turbulence and they can inhibit fluid turbulence, depending on the size of a certain eddy and the particle. A particle flowing in a fluid with certain slip velocities causes turbulence due to vortex shedding (Fig. 2.2). Small vortices separate at the surface and form a wake after the particle. Turbulence is produced by extracting kinetic energy from the fluid and one could call this augmentation of turbulence due to particles. But particles can also attenuate turbulence. If a particle is confronted with an eddy which it cannot follow, it will flow through the eddy and break it. The resulting smaller eddies will dissipate faster and in this way turbulent energy will be lowered by the particle.

Gore and Crowe [2] have defined a ratio d_p/Λ between particle diameter and the size of the energy-carrying vortex (integral length scale). If this ratio becomes larger than 0.1, the particles cause an augmentation of the turbulence,

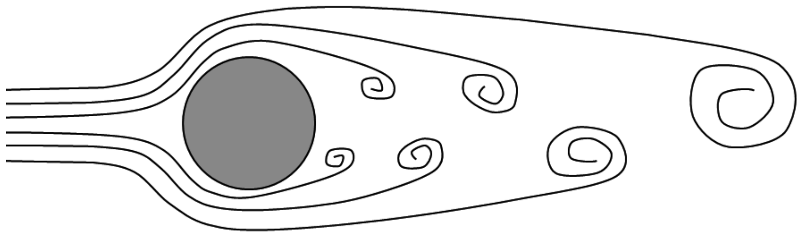

Figure 2.2: Augmentation of turbulence due to particle vortex shedding

while for values lower than 0.1 the particles attenuate the turbulence in the carrier phase. As discussed in Paper II, the value for the integral length scale varies significantly between different locations in the flow. In contrast to the Stokes number, neither the density nor the viscosity is considered in the value. The ratio d_p/Λ gives information about the size scales at which the turbulent production outweighs the enhanced turbulent dissipation.
With increasing particle concentration the particle-particle interaction becomes of more relevance. When two particles collide with each other they not only exchange momentum, but change their trajectory significantly. Particles obtain a strong component through collisions, and this is directed orthogonal to the fluid flow. Depending on particle inertia a certain distance is necessary until the particles adapt to the fluid flow direction and velocity again. During this time the particles transfer their momentum to the continuous phase. In this way, particles enhance the exchange of momentum between different regions of fluid flow and generate a much larger particle dispersion.
Gravitation is also an important factor for larger particles; solid particles will always tend to fall to the bottom of the flow configuration and the energy to lift them or keep them suspended has to come from the kinetic energy of the flow. In the present study only solid glass particles are discussed, they can always be assumed to be spherical and of identical size. Agglomeration, breakup and variation in shape can be neglected.

The collision Stokes number (equ.2.3) is the relation between the particle relaxation time and the time scale of inter particle collisions (τ_c). Crowe et al. [1] use the collision Stokes number to quantify if a particle flow is dilute or dense. In dilute flows the particle-particle interaction is of minor influence, the

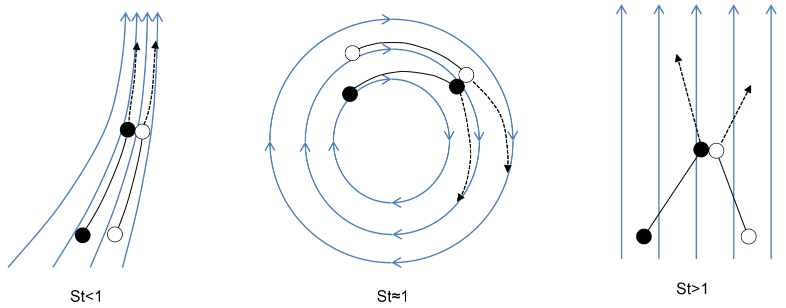

Figure 2.3: Inter particle collision behaviour with different Stoke number

distance between particles is large and collisions are rare. For all investigated flow conditions, in the mixing vessel as well as in the jet, a collision Stokes number larger than one was identified. Consequently all investigated cases can be described as dense two-phase flows. In dense flows the particle-particle interaction is not negligible. Collisions occur often and play a major role in the momentum transfer.

$$Stokes_c = \frac{\tau_p}{\tau_c} \tag{2.3}$$

The collision behaviour of particles in a viscous fluid varies with different particle Stokes numbers (Choi et al. [3]). Particles with a small Stokes number flow parallel to the fluid streamlines with a very similar velocity. Collisions between these particles happen mainly due to flow fluctuations and accelerations, while the colliding particles have similar trajectories. The particles have only a small change in trajectories after collision and shortly after will follow the fluid streamlines again (Figure 2.3). Particles with large Stokes numbers only follow the fluid flow to a certain extent; their trajectories can differ a lot from the fluid streamlines. Due to large differences in velocity and direction collisions between these particles can be very strong and cause significant changes of the particle trajectories. The particle is able to move a far distance even in directions crossing the fluid streamlines, because the particle inertia is dominant. In this way, particles can, caused by collisions, travel into different flow regions and transfer momentum to the fluid or other particles.

2.2 Flow structures in mixing vessels

2.2.1 General

Mixing is one of the most common processes in chemical engineering. There are numerous different configurations of mixing equipment for specialized purposes. Two main configurations are the axially agitated and the radial agitated mixers. In a radial agitated mixer the impeller is of the Rushton type with varying blade numbers. The fluid is discharged from the impeller in the radial direction and when impinging on the walls of the mixing vessel it splits in upwards and downwards flows. Rushton type mixing vessels are characterized by double flow loops; one upper and one lower flow loop (fig. 2.4). Axially agitated mixers have a pitched blade turbine (PBT) impeller, which discharges the fluid in the axial direction. If the impeller jet is directed downwards, a strong jet hits the bottom and splits to create a strong upwards-directed jet at the vessel walls (Hasal et al. [4]). Axially agitated mixers are characterized by this strong upwards jet and one flow loop which carries the fluid from the bottom to the surface and back into the vessel centre (fig.2.4).
Close to the impeller the flow is dominated by strong turbulence. Especially Rushton impellers produce very large shear forces at the blades, which in gas-liquid suspensions is used for bubble breakup and dispersion. Impellers with an axial discharge produce less shear, especially when the blades are airfoil shaped. All impeller styles induce a strong rotational component to the flow, which can only be broken by static baffles on the vessel walls. Baffles prevent the flow from just rotating in the vessel, but they also cause strong shear forces and turbulence.
In the study in Paper II a 45° PBT was used to stir the suspension, because the axial discharge jet has great advantages when lifting heavy particles off the bottom. The solid particles are carried upwards and dispersed by the strong jet like flow close to the baffles. The energy to lift heavy particles off the bottom and to keep them dispersed has to be taken from the kinetic energy of the flow. With increasing particle concentration the flow velocities decrease. At the same time the fluid is no longer able to lift the particles to the surface of the vessel and a cloud of particles is formed which does not fill the upper region of the vessel. This particle cloud phenomenon has been the object of numerous

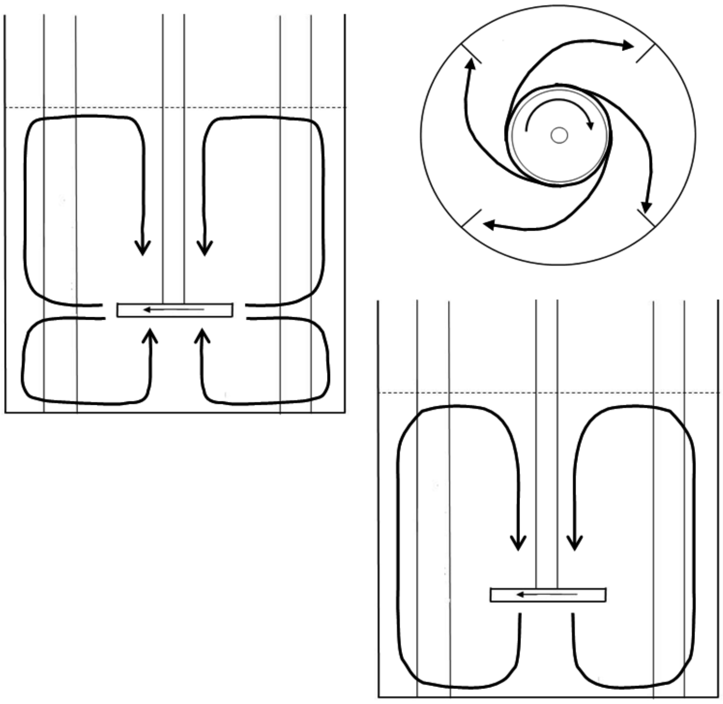

Figure 2.4: General flow in different mixing vessels

investigations, e.g., Bittorf and Kresta [5] and Bujalski et al. [6]. A often used criterion to estimate the cloud height for a certain solids loading is given by Zwietering [7].

2.2.2 Macro instability

Macro instability (MI) phenomena are large-scale flow instabilities that occur in mixing processes. The general flow field as described in 2.2.1 in a mixing tank features not only strong turbulence but also a large periodic change in flow direction and velocity. In contrast to high frequency turbulence and the high rotational speed of the impeller, an MI phenomenon is characterized by a

impeller speed in rpm	impeller freq. in Hz	MI freq. in Hz	non-dimensional MI freq.	Re
390	6.5	0.381	0.059	18,000
1,050	17.5	1.06	0.061	49,000
1,500	25	1.5	0.060	70,000
1,800	30	1.78	0.059	84,000

Table 2.1: MI frequency with varying impeller speed

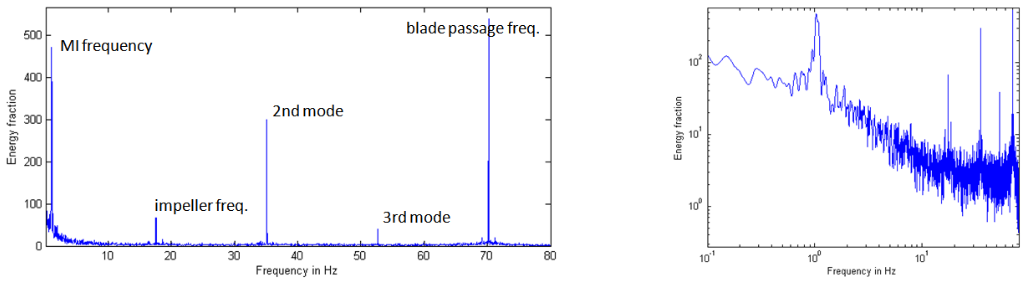

Figure 2.5: Lomb spectrogram with MI frequency and impeller frequencies in linear- and log-scaling

low frequency. MI phenomena can be recognized throughout a mixing vessel, but their dominance varies at different vessel locations (Kilander et al. [8]). The periodic change in the mixing flow plays a major role in the mixing process in the vessel. As an addition to the general flow loop, an MI phenomenon enhances the interchange of fluid packages. Yianneskis et al. [9] has described the MI phenomenon as a precession vortex around the impeller shaft.
The frequency of MI phenomena is linearly related to the rotational speed of the impeller; therefore a Strouhal number or a non-dimensional frequency is often used to describe MI phenomena.
Results obtained in the present study have been used for the following explanation of the MI phenomenon. With a frequency analysis using the Lomb algorithm 3.3.1, the energy content of each frequency in a flow can be identified. Figure 3.4 shows a typical spectrogram with a strong peak, which describes the macro instability in the flow. Table 2.1 shows the relation between the MI frequency and the rotational speed of the impeller. The non-dimensional MI frequency $f_{MI}/f_{impeller}$ was identified as 0.06. Figure 2.5 shows a spectrogram of a typical flow situation in relative proximity to the impeller in a mixing vessel. The impeller frequency can be identified as 17.5Hz and the blade passage frequency for a four bladed PBT impeller as 70Hz. The macro instability has a low frequency of only 1.06Hz in this case. Figure 2.5 also shows the logarithmic scaled version of the spectrogram, which is commonly used when analysing turbulence, but has disadvantages in a low frequency analysis.

Chapple [10] have concluded that an MI phenomenon occurs due to interaction between the impeller, the baffles and vessel geometry. Galletti et al.

[11] have found that the linear dependence between the frequency of the MI phenomena and the rotational speed of the stirrer exhibits different proportionality constants for low, intermediate and high Reynolds number flows. They have also found, using both a PBT and a Rushton turbine, that the off bottom clearance of the impeller has no significant effect on the frequency of the MI phenomena. They did however find that the frequency changed when the ratio between the impeller diameter and the tank diameter changed.

$$\tau_i = \frac{1}{f_{MI}} \tag{2.4}$$

MI phenomena are of interest especially for the dispersion of solid particles. Solid particles cannot follow fast turbulent fluctuations, but a low frequency instability is able to transport heavier solids. There are very few investigations into how MI phenomena are influenced by the presence of solids. Jahoda et al. [12], i.e., have found a significant decrease in the frequency of MI phenomena at a solids loading above 10%(w/w). Paglianti et al. [13] have investigated a concentration of 40%(w/w) and found a lower frequency of MI phenomena in the suspension than in the single-phase flow. Bittorf and Kresta [5] have observed a disappearance of the MI phenomena at high solid concentrations, which coincided with the appearance of a clearly defined cloud height. The present study tries to relate the interaction between particles and MI phenomena to the particle Stokes number (equ.2.1). As a characteristic time scale of the flow τ_i the reciprocal of the frequency of MI phenomena was used. With the definition from Equation 2.4 the particle response time was related to the time scale of the MI phenomena. For the particles used in Paper II this leads to values between 0.28 and 1.1, as shown in Table 2.2.

particle diameter in mm	particle relaxation time in s	reciprocal of MI frequ. in s	Stokes number
1	0.156	0.5618	0.278
1.5	0.351	0.5618	0.625
2	0.624	0.5618	1.111

Table 2.2: Stokes number of different particles in relation to the identified MI

2.3 Flow structures of a particle suspension jet

Jet flow is a special case of shear flow that is characterized by a very strong velocity gradient between two fluids. The most common case is an injection jet where fluid is injected at a high velocity into a stagnant fluid bulk. But jets also occur as part of more complex flow systems, such as jet mixers, the discharge jet from a mixing impeller, the flow over a step or in flows with a high velocity difference.
Due to viscous shear, momentum is transferred between a high velocity jet and the surrounding fluid. As a result the centreline velocity in a jet decreases with increasing distance from the jet origin, while the width of the jet increases. The flow has all the properties of a pipe flow at the exact location of the nozzle exit. Directly after the nozzle the jet interacts with the surrounding fluid and a shear layer develops. While the core of the jet still has the properties of the pipe flow, the shear layer between the jet and the surrounding fluid is dominated by high turbulence.
Turbulence is produced in the region of high shear by extracting kinetic energy from the main flow. High turbulence intensity indicates a large momentum transfer between fluid layers. A three-dimensional free jet typically expands with an angle of 10°, while the shear layer grows and swallows the jet core. At this point the jet becomes substantially exchanged with the surrounding fluid and has great turbulent kinetic energy; although turbulent production and dissipation are in equilibrium. At farther distance from the nozzle, the dissipation of turbulent energy takes over and the main flow decreases further until any gradient between the jet and the surrounding fluid is equalized. Single-phase jet flows have been included in many studies, some of the most famous and detailed are, e.g., by Townsend [14], Hinze [15], Wygnanski and Fiedler [16] and Gore and Crowe [2].

Influenced by external factors, a jet can become unstable Batchelor and Gill [17]. After a certain distance from the nozzle, the jet starts to fluctuate around the centreline and the flow becomes dominated by large-scale vortices. The large-scale vortices of the jet instability significantly enhance the exchange of momentum and mass, and the surrounding fluid is entrained into the main

flow. This instability is of importance particularly when considering the mixing behaviour of a solid-liquid suspension. The large-scale vortices are slow and particles in a suspension are able to follow them, which significantly increases the dispersion.
Particles of different sizes affect a flow differently and the relations of the flow to length and time scales are important. Particles influence, as described in 2.1, the turbulent structures of a fluid flow. By breaking bigger vortices into smaller eddies turbulent kinetic energy is dissipated faster, but particles can also add turbulence to a flow. These influences on the energy cascade of turbulence affect the transport of momentum, mass and heat. Many studies have been investigated the influence particles have on a jet in gas-solid suspensions, but only very few have investigated solid-liquid suspensions.

Most studies have concluded that particles in a gas flow enhance the experienced viscosity, and that the axial flow profiles are flatter and the decay of centreline velocity decreases, e.g. Fan et al. [18] and Sheen et al. [19]. Gore and Crowe [2] have suggested that an augmentation of turbulence occurs due to particles when the ratio between the particle diameter and the integral length scale (equ.3.8) of the flow is larger than 0.1; in contrast particles cause an attenuation of turbulence at a value smaller than 0.1. While the integral length scale refers to the size of the energy-carrying eddies, the Stokes number also includes the viscosity and the density difference between particle and fluid. Identifying the characteristic time scale of the flow in a jet is not possible without measurements. Therefore Hardalupas et al. [20] have defined a semi-empirical formulation to determine the particle Stokes number at different flow conditions as a function of the distance from the nozzle (equ. 4.1). They have described an increase in Stokes number with increasing nozzle distance, which is connected to the decrease in flow speed and the increase in the size of eddies. A change in Stokes number means that the particle influence differs by distance from the nozzle. Parthasarathy [21] have investigated how particles influence the instability of a gas-solid jet. They found a decreased instability frequency and a flow stabilizing effect due to particles.

3

Experimental

3.1 Equipment

3.1.1 Paper I - Mixing vessel

The study of a particle-laden flow in a mixing vessel was conducted in a model made completely of glass. The flat bottomed cylindrical tank had a diameter of T=150mm and was filled up to a height equal its diameter T=H. The suspension was axially agitated by a 4 bladed 45° PBT with a diameter of D=T/3 and no hub. The tank was equipped with 4 baffles with a width of B=T/15=10mm. The impeller rod, the blades and the baffles were made of steel. The ground clearance of the impeller was kept constant at C=T/3. The convex surface of the cylindrical vessel is problematic when conducting measurements with an optical technique such as LDV. To prevent the laser beams from attacking from an angle that is too steep, the tank was placed in a square glass tank filled with water. This ensures an attack angle of 90° on the glass surface and only a small refraction to be overcome when the beam enters the mixing vessel.
Measurements at 18 different locations, separated into two vertical rows at 9 locations, were conducted in this study. The measurements #001 - #009 were located in the vessel bulk at half the radius of the vessel centreline. The measurements #010 - #018 were located close to the vessel wall on the windward side of the baffle, where the strongest influence of MI phenomena was expected. Figure 3.1 shows the setup and the measurement locations in the mixing vessel.

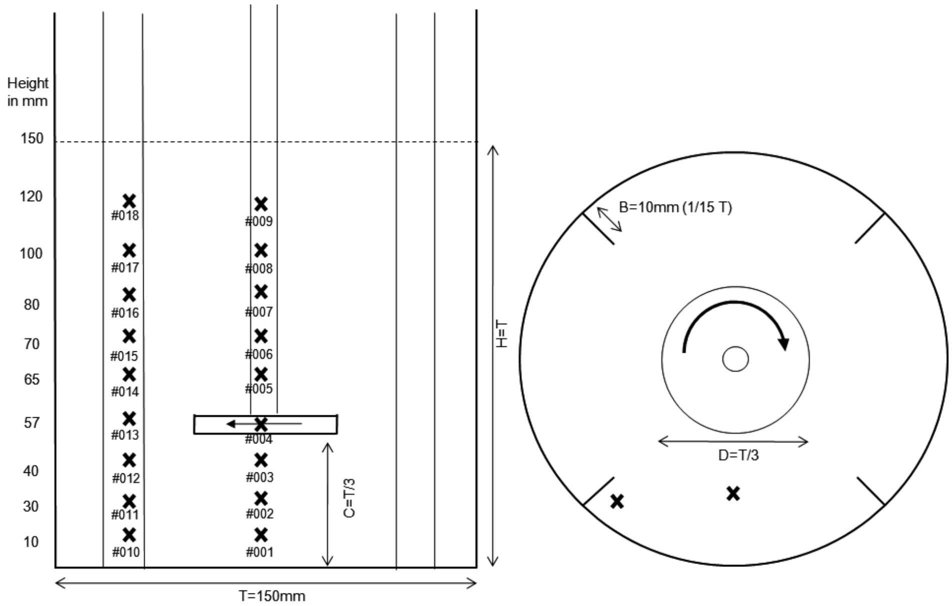

Figure 3.1: Measurement configuration of the mixing vessel

3.1.2 Paper II - Confined jet

Studying the flow properties of gaseous jets is usually done in radially symmetric jets injected into free space. Dealing with a liquid flow medium is by far more difficult. The liquid medium has to be pumped in a loop, all components have to withstand the water pressure, and the tank dimensions are somewhat limited in size. It is therefore not feasible to study a radially symmetric jet, but rather a jet confined between two narrow walls in one direction while free to expand in the lateral and axial directions. When adding particles to a liquid flow loop the possibility of particle accumulation in the equipment has to be considered. Buffer tanks, horizontal pipe sections and flat bottomed tanks are not applicable.

For the confined jet study in Paper II, a special tank was constructed to satisfy all the demands of the optical measurement technique and the used suspension. The equipment is comparable in all geometrical aspects to the equipment used by Virdung and Rasmuson [22]. A large glass tank with the measurements 1000mm*900mm comprised the centre part of the setup; the suspension was injected through a square nozzle (17mm) 100mm under the liquid surface (fig. 3.2). With a depth of only 20mm, the tank was only 1.5mm

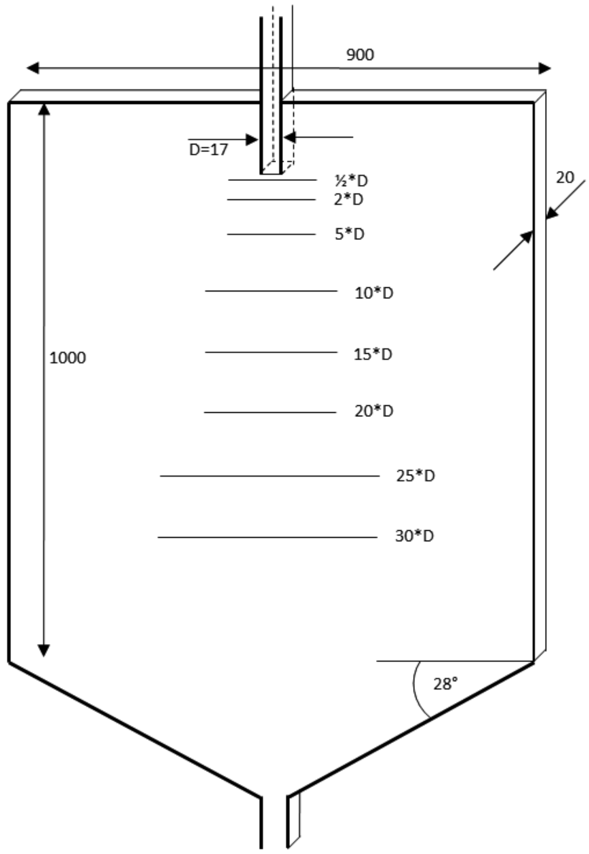

Figure 3.2: Measurement configuration of the confined jet

wider than the nozzle on each side. This way the jet was constrained in its expansion and the lateral and axial flow components dominated. Although the average flow in the constrained direction might be zero, flow turbulences were three-dimensional and fluctuations in the constraint directions were not completely negligible, but were expected to be minor.
The tank was completely filled with water, equipped with a lit and ventilated by a small opening. The tank was completely made of glass to maintain optical accessibility. To prevent particles from accumulating in the tank, the bottom was conically shaped with an angle of 28° and led directly into the pump. All pipe sections were designed to avoid horizontal parts. The suspension was continuously pumped by an excenter screw pump in a closed-flow loop without further buffer tanks. This can cause unwanted flow disturbances originating from pump fluctuations, but was necessary to maintain a constant particle concentration in the inlet nozzle. Certain frequencies due to pump rotation

and vibrations were registered in the spectrograms close to the nozzle, but disappeared at farther axial distances.

3.2 Laser Doppler Velocimetry - LDV

Most measurements presented in this thesis were obtained by means of (laser Doppler velocimetry) LDV. LDV is a non-invasive optical measurement technique to determine velocities Durst et al. [23]. The LDV system used in the studies was a commercial system from Dantec Measurement Technology; the FiberFlow dual beam system (Series 60X). Figure 3.3 shows a schematic view of the LDV setup. The light source was a Spectra-Physics water-cooled 6W Ar-ion laser model Stabilite2017. In the transmitter unit the laser light was split into two beams and separated into the three most dominant wavelengths. In the setup for the mixing vessel (Paper I) only one wavelength (514.5nm) was used, while in the study of the confined jet two wavelengths (514.5nm and 488nm) were used.

Fibre optics transported each beam to the main LDV probe, from there they were guided into the measurement section. The two beams of the same wavelength (same colour of light) crossed at 310mm from the lens in the focal point. All beams were focused with an expansion factor of 1.98, so that the intersection volume, which forms the measurement volume, was kept as small as possible. A small measurement volume guaranteed a large spatial resolution and yielded, in this case, a volume length of 702 microns and a diameter of 76 microns. The intersecting beams formed an interference pattern of dark and bright zones, so called fringes. LDV cannot measure velocities of perfectly clear fluid; consequently small tracer particles are needed. Dantec 9080A7001 silver-coated hollow glass spheres with a diameter of 10 microns and a density of density of $1.3kg/dm^3$ were used in this thesis. They were small enough so their inertia could be negelected and their velocity was assumed as equal to the liquid flow. When a tracer particle that is sufficiently small flows through the measurement volume, it reflects the dark and bright zones.

Depending on the velocity of the tracer, a reflection function, a so called burst, can be received. The probe also functions as a receiving unit, which means that the LDV was operated as a backscatter system. The light received by the probe

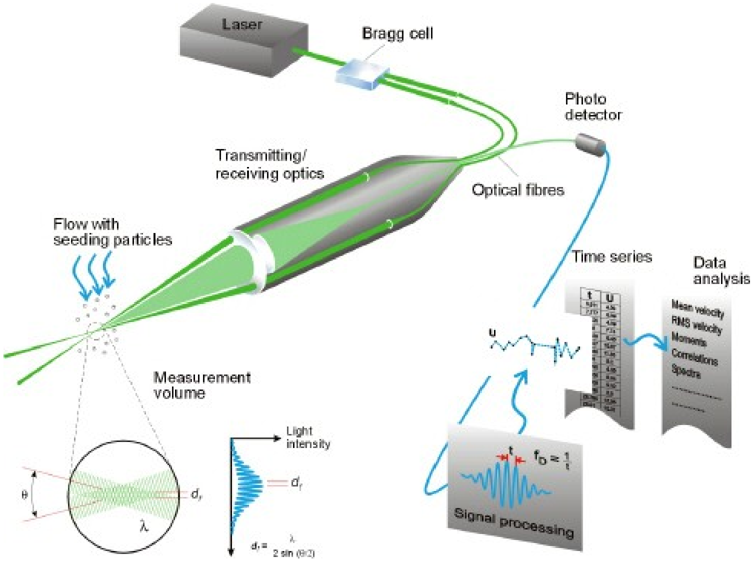

Figure 3.3: Principle of laser Doppler velocimetry - ©Dantec Dynamics

was split into the different wavelength components again and the light of each wavelength was sent to a photo multiplier where the light signal was converted into an electric signal. The electric signal was processed in a burst spectrum analyzer (BSA). The BSA separated valid tracer bursts from the background noise, and each burst signal was stored as a velocity value.

In the interference pattern of two laser beams, only the velocity perpendicular to the fringes can be determined, which is related to only one flow component. If a second velocity component is desired, an additional pair of beams must be used to create an interference pattern perpendicular to the first one, but at the same intersection point. To be able to separate reflected light from both components, light with different wavelengths was used for each pair of beams. In Paper II, for example, light with a wavelength of 514.5nm was used to measure the axial velocities in the jet and a wavelength of 488nm was used to measure the lateral velocities. To be able to measure flow with zero velocity and to alternate between positive and negative flow directions, the interference patters were constantly moved at a speed much higher than the expected flow. The movement of the interference pattern was achieved by shifting one beam of each pair by a frequency of 40MHz.
The data including the arrival time, transit time and velocity of each tracer de-

tected were sent from the BSA to the windows-based BSA flow software, version 2.12.00.15. The software allowed for the monitoring of ongoing measurements and controlling the measurement setup including the measurement locations. To maintain a high data rate, the data obtaining settings of the BSA have to be adjusted to the predominant measurement conditions. The high voltage going to the photo multiplier can be adjusted to increase the electric signal, but this will also increase existing noise, while the signal gain amplifies signal peaks. For measurements in the mixing vessel a signal gain of 44db and a high voltage of 1,216 V was chosen, while a signal gain of 32db and 1,567 V as high voltage were used in the flow measurements in the confined jet.
The velocities of large particles in the solid-liquid suspensions will be different from the fluid velocity. Therefore it has to be observed with care that the LDV does correctly separate between signals received by the tracers and reflections from the particles. In the suspensions investigated, the particles were dimensions larger than the tracers and also larger than the diameter of the measurement volume. In this case, the reflection from a particle looked significantly different than the one from a tracer. While a tracer reflects the interference pattern, larger particles will solely reflect the average light intensity. The BSA is able to separate these signals and exclusively allow valid bursts from the tracer by using the oversize rejection setting. More detailed information can be found in the principles and practice of laser-Doppler anemometry, Durst et al. [23].

3.3 Data processing

3.3.1 Lomb algorithm

The LDV measures instantaneous velocity values with a very high data rate. In instationary flow situations this gives a temporal distribution of the velocity at each location. Besides the average velocity this also contains information about turbulent kinetic energy, vortex length scales and periodic flow phenomena.
There are two common ways for analysing frequency spectra; either using the Fourier transform or using the Lomb algorithm Lomb [24]. The LDV detects a velocity value the moment a tracer flows through the measurement volume.

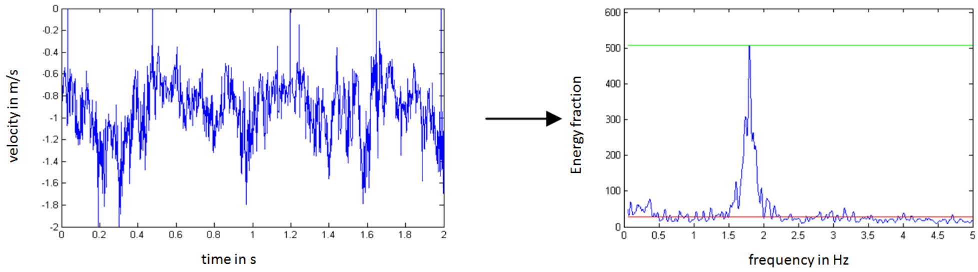

Figure 3.4: Analysis of typical velocity data into a frequency spectrogram

This occurs randomly distributed around the average data rate. LDV data, in contrast to hotwire or PIV measurements, are not obtained with a fixed temporal resolution, but instead have an unequal temporal distance between measured values. The Fourier algorithm requires equally spaced data, however, which would make it necessary to resample the LDV data by deleting values and filling gaps by estimated ones. The Lomb algorithm is able to handle non-equally spaced data, can handle the raw data from the LDV and was therefore used throughout this work. For the input data h the Lomb algorithm becomes Press et al. [25],

$$\langle h \rangle = \frac{1}{N} \sum_{i}^{N} h_i \tag{3.1}$$

$$\sigma^2 = \frac{1}{N-1} \sum_{1}^{N} (h_i - \langle h \rangle)^2 \tag{3.2}$$

$$\omega = 2\pi f \tag{3.3}$$

$$\tan(2\omega\tau) = \frac{\sum_j \sin 2\omega t_j}{\sum_j \cos 2\omega t_j} \tag{3.4}$$

$$P_N(\omega) = \frac{1}{2\sigma^2} \left\{ \frac{\left[\sum_j (h_j - \langle h \rangle) \cos\omega (t_j - \tau)\right]^2}{\left[\sum_j \cos^2 \omega (t_j - \tau)\right]} + \frac{\left[\sum_j (h_j - \langle h \rangle) \sin\omega (t_j - \tau)\right]}{\left[\sum_j \sin^2 \omega (t_j - \tau)\right]} \right\} \tag{3.5}$$

The probability of $P_N(\omega)$ between i and $i + di$ is $e^{-i}di$ So if we look at M independent frequencies the probability that none of them gives a larger value (i) is $(1 - e^{-i})^M$. One disadvantage of the Lomb algorithm is that it is compu-

tationally heavier than the FFT and the amount of operations scale with the number of data points, N, as N^2. The in-house code was based on the C code given by Press et al. [25] and written in Matlab R2011 in order to calculate the Lomb spectrogram.
Figure 3.4 shows a typical velocity plot as obtained by the LDV, and the corresponding spectrogram after Lomb analysis. Already in the velocity plot a certain periodically large fluctuation can be identified. In the spectrogram this appears as a clear peak with a low frequency. The energy fraction inherent to each frequency of the flow was analyzed with the Lomb algorithm and illustrated in a spectrogram. Dominant frequencies in the flow will contain a large fraction of the energy and therefore cause high amplitude in the spectrogram. Thus, periodic flow phenomena can be identified and their strength can be evaluated.

3.3.2 Signal to noise ratio

The amplitude in the Lomb spectrogram gives a measure of the energy fraction of each frequency in relation to the flow energy. With a spectrogram, one can identify dominant flow frequencies, periodic phenomena and the energy dissipation of turbulences with high frequencies. The absolute amplitude in the spectrogram is not suitable for qualitative evaluations of the strength of a periodic phenomenon when comparing different measurement conditions.
A measurement series was conducted in which the physical flow conditions and measurement location were maintained while the measurement parameters, such as laser power or signal gain were varied in order to manipulate the data rate of the measurements. The investigated instability could be identified at identical frequencies under all measurement conditions, but the maximum amplitude did show a notable dependence on the data rate. To be able to compare the strength of instabilities in different suspensions, an analysis method is needed which is independent of the measurement data rate. This is especially needed when investigating suspensions with different concentrations of solids, because denser suspensions create less perfect conditions for the LDV consequently causing a lower data rate.

A solution to this problem is to use the ratio between the maximum peak amplitude and the average background noise of each measurement. It was recognized that when the maximum amplitude of a peak decreased due to a low data rate, so did the amplitude of the background noise. In all further analyses the ratio between the maximum peak amplitude and background noise was used as a measure of the level of dominance of a periodic phenomenon. The signal to noise ratio was proven to be a feasible analysis technique to compare the strength of instabilities despite varying measurement conditions.

3.3.3 Moving average RMS

To investigate the turbulent kinetic energy of a flow, all three flow components must be measured. The used setup limited the number of measurable components to two, so it was not possible to gain direct access to the total turbulent kinetic energy. But particularly in the confined jet flow it was of interest to obtain information about turbulence in the flow. Therefore the root mean square (RMS) of the obtained two flow components was determined only as shown in Equations 3.6 and 3.7.

$$RMS = \sqrt{\frac{1}{2}\overline{\left(v'_{axial}\right)^2} + \overline{\left(v'_{lateral}\right)^2}} \tag{3.6}$$

$$with \qquad v\left(t\right) = \overline{v} + v'\left(t\right) \tag{3.7}$$

The described RMS value includes the axial and lateral components of the fluctuations in the same way as the definition of the turbulent kinetic energy, but without considering the third flow component. Although the flow is confined in the third component and has no average velocity, the fluctuation velocities will be non zero, and isotropic turbulence cannot be assumed. However, the fluctuation energy in the confined flow component is significantly lower than in the axial and lateral components and is not expected to add any information of interest to the evaluation. Therefore the RMS value is assumed to be representative of the overall turbulent kinetic energy in the liquid flow of the jet in Paper II.

In flow configurations with an instationary flow, the time dependent average velocity must be considered when determining the fluctuating velocities v'. A similar problem occurs when the flow is dominated by a large-scale periodic phenomenon. An overall time averaged mean value would produce large fluctuation velocities, hence high RMS values. To avoid artificially increased RMS values, a moving average was applied as a contrast to an overall average. The moving average was calculated in blocks of constant time. With the Lomb spectrogram the frequency of the large-scale periodic instability could be determined, and a block size could be chosen. A block size of 0.25s was chosen for the confined jet, because the frequency analysis showed that it would be a good compromise between filtering large-scale movements and mapping turbulent kinetic energy.

3.3.4 Integral length scales

Turbulent flow can be characterized by the different length scales of the flow. The small length scales, such as the Kolmogoroff length scale, describe the size of the smallest eddies before they dissipate into heat due to viscosity. These small length scales are of importance when modelling a turbulent flow and when studying the dissipation rate of turbulent energy. The present study focuses on the interaction between comparably large particles and the fluid. Large and heavy particles are not influenced by the small eddies of the flow, but rather by flow instabilities and large-scale vortices. Therefore it was of interest to study the Taylor macro scale Λ (Taylor [26]), who has described it as the size of the eddies carrying the most energy.

$$\Lambda = v_{convective} \int_0^\infty R(\tau)\ d\tau \tag{3.8}$$

$$R(\tau) = \frac{1}{v'(t)^2} \int_0^\infty v'(t)\, v'(t-\tau)\ dt \tag{3.9}$$

The method for directly determining the integral length scale (equ.3.8) would make use of the spatial correlation, which would demand simultaneous measurements at different locations. This cannot be achieved with the used setup. With the LDV, one point measurements of two flow components with a very high temporal resolution are obtained. Therefore calculations here are based on the temporal autocorrelation (equ.3.9) at each point to determine the Eulerian integral time scale, which multiplied by the convective velocity gives the integral length scale Hinze [15].

3.4 Experimental procedure

3.4.1 Paper I

In addition to a single-phase case, suspensions with particles of different size and concentrations were investigated. Water was used in all cases as the liquid phase and spherical glass particles with a density of 2.5kg/dm3 were used as the solid phase. Particles with a diameter of 1mm, 1.5mm and 2mm were used in separate studies, the concentration was stepwise raised in order to investigate 17 different volumetric concentrations between 0%vol and 11.8%vol. Due to the decrease in penetration depths for the laser beam at high concentrations, it was only possible to conduct measurements up to 7.4%vol at positions deep in the vessel, #001 - #009 (Fig. 3.1).
The impeller speed was not changed during this study and in all setups the suspension was agitated with 1800rpm(30rps). A high rotational velocity was needed to lift the particles off the bottom. The criterion by Zwietering [7] for particle suspensions confirms the visual observations that 30rps are sufficient for all suspensions except the highest concentrations of the 1.5mm and 2mm particles, where 34rps are needed. At these concentrations stagnating particles could be observed on the bottom and on the windward edge between the baffles and the vessel wall.
The LDV was operated in single-burst mode and for each position a constant amount of 200,000 samples was acquired. The signal gain was set to 44dB and the high voltage to 1,216V. The laser power was varied to keep the data rate as stable as possible for all measurement conditions, but with higher solid loading a drop in the data rate was inevitable. The change in data rate caused a change in data acquisition time, which varied between 71.4s and 2,000s, relating to 127 and 3,560 periods of the determined MI phenomenon.

3.4.2 Paper II

In the study of particle influence on the turbulence structures in a jet, suspensions with three different kinds of particles were investigated. In all suspensions water was used as the liquid phase and solid glass particles with a density of 2.5kg/dm3 were used as the solid phase. The smallest particles had a diameter of 0.5mm, the bigger ones 1mm and the largest particles 2mm. Different volumetric concentrations of solid particles were investigated; the maximum concentration was 6.3%vol for the 1mm particles and 2.5%vol for the 0.5mm particles. To obtain the particle concentration in a jet, a sample was taken from a valve in the inlet pipe. The total weight of the sample was compared with the weight of the solid phase after vaporizing all water. The concentration was calculated in volumetric units independent of particle size.
With the two-component LDV the velocities of the liquid phase in the axial and lateral directions were measured. To obtain information about the average velocity, turbulences and large-scale instabilities, measurements were sampled for 120s at each location. The measurement locations were organized in eight horizontal lines with increasing distance from the nozzle. All lines were located in the centre plane of the tank. The measurement locations are further described in Figure 3.2. With the eight different lines, the flow profiles of velocity, the RMS and the integral length scale could be determined.

4

Results and discussion

4.1 Paper I

The velocity measurements conducted in the mixing vessel showed the strong periodic behaviour of a non-dimensional frequency of Strouhal=0.06. At an impeller speed of 30Hz this led to a frequency of 1.78Hz, which was identified as an MI phenomenon (Table 2.1). The measurements were taken at 18 different locations in the vessel (Fig.3.1) and the Lomb spectrograms were analysed for all measurements. MI phenomena could be found in all measurements, but the strength varied between different locations. At the locations #010-#018, on the windward side of the baffle, the strongest influence of MI phenomena could be identified. Suspensions at 11 different concentrations of particles of three different sizes were investigated in this study.
As mentioned in Chapter3.3.2, it proved to be difficult to compare the strength of the MI phenomena between different setups of different locations in the vessel. Therefore the ratio between the max amplitude of the MI and background noise was used to determine the strength of the MI. A number of test measurements were conducted to inspect the stability of the measured results. The sensitivity of the analysis reaction to variations in the data rate, sampling time and number of samples was tested; the dependency of the results was also tested for different settings of the LDV technique, such as the oversize rejection value, the burst detection criterion or quality factor. It was found that the frequency of the MI phenomena was determined as Strouhal=0.06 under all conditions,

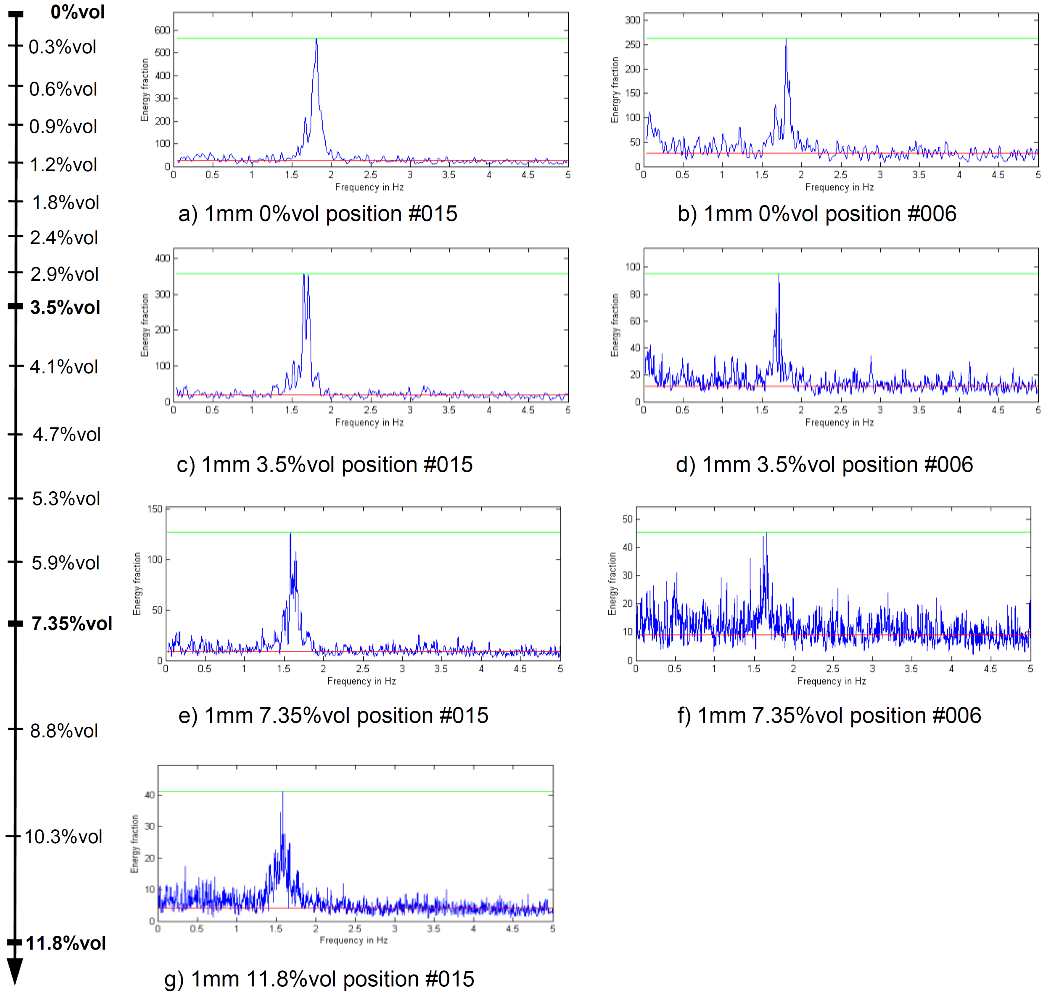

Figure 4.1: Lomb spectrograms for different locations in the mixing vessel by increasing particle concentration

but the maximum amplitude of the MI showed a certain sensitivity to the data rate and the total time of sampling. The signal to noise ratio, on the other hand, showed better consistency in determining the strength of the MI.

Figure 4.1 shows the Lomb spectrograms from the suspension with 1mm particles. One measurement position close to the baffle (#015) and one measurement position in the vessel bulk (#006) were chosen to be presented in the figure. The results are representative for all other measurements. The single-phase case was re-measured for all three particles to rule out variations in the setup when changing the suspensions. At locations deep in the vessel it was not

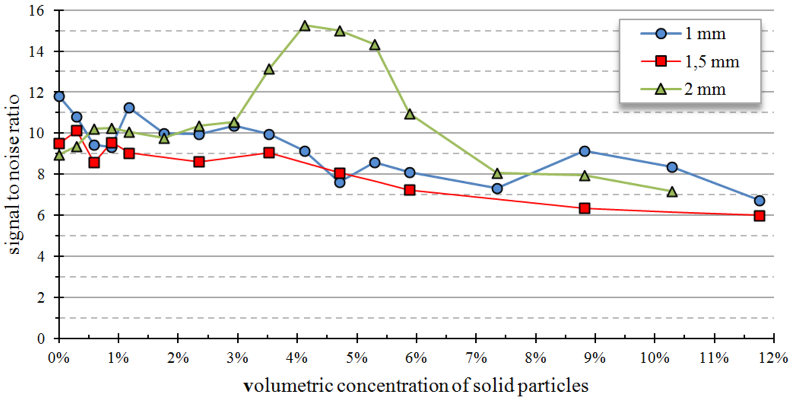

Figure 4.2: Amplitude of the MI with increasing particle concentration

was not possible to measure concentrations greater than 7.35%vol, while at the baffle a concentration of 11.8%vol could be measured (Fig. 4.1). It can be seen that the MI peak remains constant at the same frequency for all concentrations investigated. But while the value of the frequency of the MI remains constant one can identify a weaker dominance of the MI in relation to background noise. Even though the strength of the MI decreased with increasing solid concentration, it could still be clearly identified at the highest measurable concentration.

The results obtained with the 1.5mm particles showed the same behaviour as the 1mm particle suspension. The suspension with 2mm particles, on the other hand, did not show a constant decrease in MI strength, but rather an increase at moderate concentrations followed by a decrease. Figure 4.2 shows the signal to noise ratio of the MI with increasing particle concentration. Each point in the chart was obtained by averaging over all 18 measured positions. Between 3%vol and 6%vol the 2mm particle suspension was characterized by a stronger MI than in the single-phase case. The increase in MI strength was observed at all 18 positions, but was the strongest at the locations #015 - #017. The increase in MI strength coincided with the formation of a clear cloud height at 2/3 of vessel height. It was assumed that the different behaviour of the larger particles was related to the larger Stokes number. For the 2mm particles a value of Stokes=1.1 was determined, while the smaller particles had values of 0.2 and 0.6 (Table 2.2). The cloud height quickly decreased to 1/2 of vessel height when the concentration was increased. The kinetic energy of the flow was not sufficient to lift all particles. The flow above the cloud was free of particles and nearly stagnant. The energy to keep the particles lifted was taken from the fluid flow, so that the flow above the cloud appeared to be cut off from the mixing flow. The cloud height was not stationary, but was characterized by strong periodic fluctuations. Only the upwards jet from the windward side of the baffles (Figure 2.4) penetrated the cloud and transported particles into the upper part of the vessel. The jet also periodically fluctuated in strength as part of an MI. The suspension with the larger particles had a strong abrasive behaviour. Significant abrasion occurred at the impeller blades and at the baffles due to collisions with particles.

Visual observations of the particle dispersion showed that collision behaviour of particles differs between more and less dense suspensions. In less dense suspensions particles travel a far distance after a collision and disperse in the vessel. Especially collisions with the impeller blades and the vessel bottom cause a very strong rebound. Particles also collide with each other, and have enough space to travel a significant distance with the post-collision trajectories. In more dense suspensions the free space between particles is very limited. If the trajectory of a particle differs from the flow streamlines after a collision, it has no space to travel before colliding with another particle. The particle trajectories are less random and the particles move in a collective manner. This way the particles don't disperse in the same manner as in less dense suspensions. The particle flow is more homogenous and behaves like a continuum similar to dense granular flows. The flow of the particle phase is significantly influenced by the momentum transfer due to inter particle collision.

4.2 Paper II

Different particle suspensions were investigated in a confined jet setup to study the effect of solids on turbulence structure and flow instabilities. The axial and lateral components of the fluid velocity were measured at 162 locations of the confined jet. Particles with a diameter of 0.5mm, 1mm and 2mm were used as the solid phase. The obtained flow profiles were analyzed for axial velocities, RMS values as well as integral length scales and dominant flow frequencies.

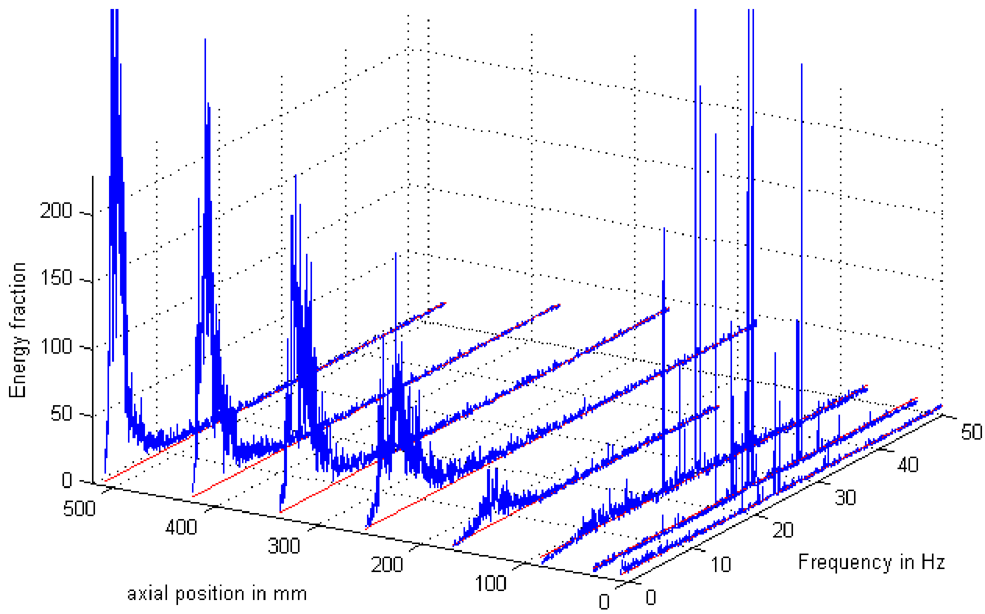

Figure 4.3: lateral Lomb spectrogram of centreline positions in single phase

The analysis of the single-phase jet clearly showed two regions of the jet. Close to the nozzle, where the jet was characterized by a stable shear layer and farther from the nozzle, where the instabilities dominated the flow. The jet became unstable after a distance of approximately 10 times the nozzle diameter (10*D). In this region the flow was dominated by large-scale fluctuations with a low frequency. Figure 4.3 shows the Lomb analysis of the lateral flow component at the centreline positions. At short distances from the nozzle the Lomb spectrograms only showed peaks at frequencies related to vibrations and the rotation of the screw pump. With greater distance a strong peak at low frequencies was recognizable. The low frequency peak at 5Hz - 2Hz was the instability of the jet. The analysis of the axial flow component showed the same behaviour, but less pronounced due to the high axial velocity. The frequency, the spatial resolution and strength were the same for the single-phase jet as for the suspension with 0.5mm and 1mm particles. The 2mm particle suspension, on the other hand, showed greater stability in the jet. While the frequency remained the same, the strength decreased and the instability occurred at a greater distance from the nozzle.

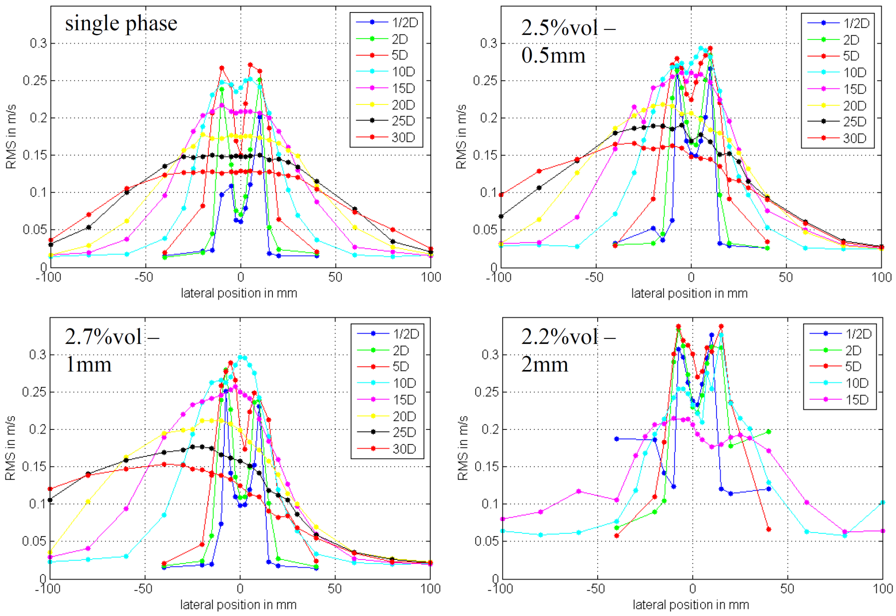

Figure 4.4: RMS profiles of suspensions with different particles

Figure 4.4 shows the RMS profiles of the single-phase jet in a comparison with the three different particle suspensions. The shear layer dominated flow is clearly identifiable with the typical double peak, while the flow farther from the nozzle is characterized by flatter and wider profiles. The presence of the particles caused higher RMS values in the region close to the nozzle. The exchange of momentum in the shear layer and the jet core increased. The RMS profiles for the 2mm particle suspension do not go down to zero outside the jet, but rather show very high RMS values in regions where the average flow is already zero. This is caused by particles that leave the jet due to collisions and carry their momentum into the fluid bulk outside the jet. The 2mm particles are largely influenced by particle collisions and particle inertia. The 1mm particle suspension was measurable up to a concentration of 6.3%vol. Significantly higher RMS values closer to nozzle were observed while the RMS profiles farther away from the nozzle were lower. This is in good agreement with the definition of the particle Stokes number in a jet by Hardalupas et al. [20] (Equation 4.1). With greater distance from the nozzle the particle Stokes number decreases and particles can better follow flow structures. Gore and Crowe [2] has described that large particles augment turbulence to the flow, while small particles attenuate turbulence. A variation in flow length and time scales also

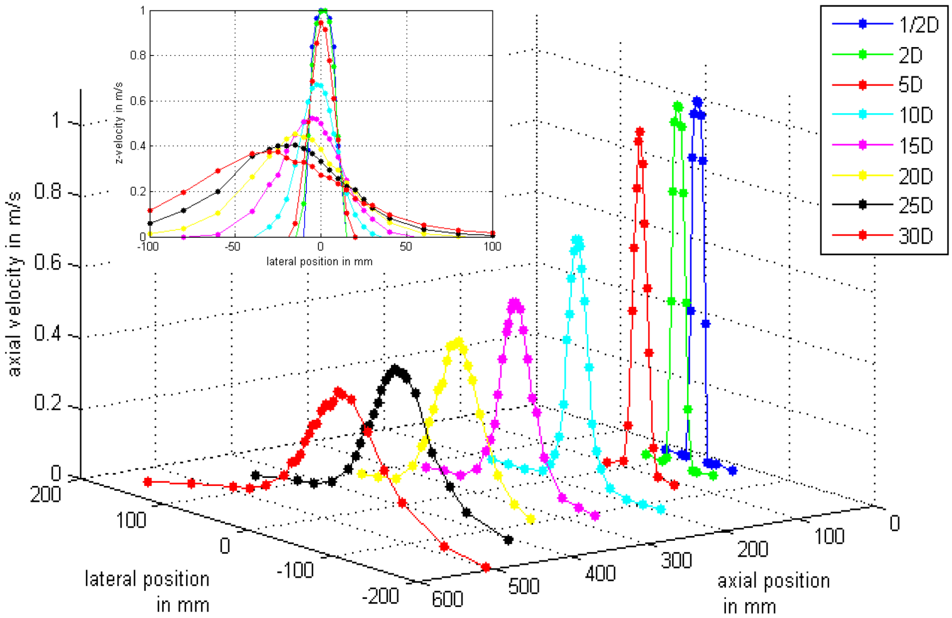

Figure 4.5: Axial velocity distribution at 2.2%vol of 0.5mm particles

means that the same particle can be small in relation to the flow scales in one region and large in another. The integral length scales d_p/Λ (Equation 3.8) at the centreline positions increase linearly with the distance from the nozzle. The values obtained in the measurements are in good agreement with the description by Wygnanski and Fiedler [16] of a gaseous jet. The presence of solid particles has only a minor influence on the integral length scales with no clear trend. For the 2mm and the 0.5mm particles a slight decrease was found while the integral length of the 1mm particle jet was identical to the single-phase case. The profiles of the integral length scale have a shape similar to the RMS distribution. This is in good agreement with the findings of Benayad et al. [27], that the integral length scale is maximal in the shear layer.

$$S = \left(S_e \frac{1}{6.57} \left(\frac{x}{D} \right)^2 \right)^{-1} \tag{4.1}$$

$$S_e = \frac{D/U_0}{\tau_p} \tag{4.2}$$

The axial velocity profiles did not show any significant difference between the single-phase jet and the different particle suspensions. Figure 4.5 shows the axial velocity profiles of the flow with 2.2%vol of 0.5mm particles. The axial profiles did not indicate a changed in the decay of the centreline velocity nor a change in jet width. While the single-phase jet was stable at the centreline, a greater tendency to diverge from the centreline was observed in particle suspensions. The jet containing the largest particles, 2mm, did not show this behaviour and was stable at the centre position even at 4.5%vol. The 1mm particle flow only showed a minor tendency to diverge from the centreline and only at very high concentrations (larger than 4%vol). With the smallest used particles of 0.5mm the jet showed a strong tendency to leave the centreline position. With a higher solid concentration the jet was more likely to diverge, which made it impossible to produce reliable measurements of concentrations exceeding 2.5%vol. The jet did not show a preferred direction, diverging to the right or to the left was equally as common. The cause of this phenomenon was most likely asymmetric disturbances inside the tank. While the single-phase jet remained stable, the particle suspension was more sensitive and enhanced the disturbance so that the jet diverged. Similar to the study in the mixing vessel, the particles ground the steel surfaces. Especially the largest particles caused significant abrasion. This caused a problem with visibility due to steel dust in the suspension and made LDV measurements increasingly difficult.

Visual observations of the flow showed that the collision behaviour varies between different particles and different concentrations. Large particles feature strong collisions with post-collision trajectories which cross the fluid streamlines. In the region close to the nozzle this leads to the effect that particles are transported out of the jet due to collisions in the jet core. Particles with a large Stokes number can be dispersed a far distance and carry momentum into different flow regions. Smaller particles are more affected by the fluid flow, they are not able to travel longer distances against the fluid streamlines. The particle dispersion is mainly due to fluid vortices and less due to collisions.
The collision effects as well differ between more or less dense suspensions. In less dense particle suspensions the particles can travel a farther distance after a collision before colliding again. After a collision the two particles travel into different flow regions and transfer their momentum to the fluid. In denser particle suspensions the particles are limited in their freedom to move. Short

time after a collision they collide again and transfer their momentum to other particles. The overall particle flow is more homogeneous and all particles have more similar vectors.

5

Conclusions and Outlook

This study has shown that it is possible to measure solid-liquid suspensions with LDV in very good temporal and spatial detail. The measurements have shown to be reliable and allow comparison between different conditions. With LDV it is possible to determine velocity distributions at very high solid concentrations and the Lomb algorithm serves well to analyze dominant frequencies in the flow. The maximal peak height received from the Lomb spectrogram was not sufficiently meaningful to make a quantitative interpretation of the amplitude of MI phenomena under different solid loading conditions. The amplitude over noise value, defined as the ratio between absolute amplitude and the average strength of the background signal, was introduced in the present study. This amplitude over noise value is much less sensitive to changes in the data rate and makes it possible to determine the significance of the frequency of MI phenomena in relation to the general flow. The study in the mixing vessel showed that the amplitude of MI phenomena, but not the frequency, was influenced by the addition of solids. A higher solid concentration showed a decrease in MI dominance. Different locations in the vessel experienced this decrease at different rates, but it could be found at all locations. Nevertheless, MI phenomena could still be identified under the maximal measurable solid concentration of 11.8%vol. Particles with a diameter of 1mm, 1.5mm and 2mm were used to investigate the possible impact of the particle Stokes number. For the 1mm and the 1.5mm particles a slow but steady decrease in MI strength was observed. However, the suspension with 2mm particles was characterized by a significant increase in MI strength between 3%vol and 6%vol. The particle Stokes number of the 2mm particles, in relation to the time scale of the MI, was 1.1 which indicates strong interaction.

Two regions could be identified in the jet flow in which the flow was dominated by different phenomena important to the transport of particles. The region in the vicinity of the nozzle features high flow velocities and a well defined shear layer with high turbulence. The flow was characterized by a small integral length scale and a large particle Stokes number in this region. The region farther away from the nozzle was dominated by large fluctuations; jet instabilities. Particles could follow these large scale vortices well, as described by the low particles Stokes number in this region. In fact it could be seen that the jet instability was the main cause for the lateral distribution of solid particles into the fluid bulk. The Lomb frequency analysis gave a good overview of the dominant frequencies and their spatial distribution in the flow.
The 0.5mm and 2mm particles acted turbulence enhancing already at relatively low concentrations. Especially in the local minimum of the RMS profiles, which describes the core of the jet, a significant increase was recognizable. The highest solid concentration was achieved with the 1mm particles. An increase in RMS at the core of the jet and in the jet shear layer was observed in the region close to the nozzle. A decrease in RMS values was measured at very high concentrations in the region of the jet instability. With an increase in particle size an increase in their effect on RMS values could be observed. The frequency spectra of the flow and the strength of the large-scale instabilities were only affected by the suspension with the 2mm particles. The 2mm particles had a stabilizing effect on the jet and caused the instability to move farther downstream, while the frequency remained the same. The axial velocity of the flow did not show any significant changes due to particles presence. No difference in the centreline velocities or jet width was recognizable in any of the suspensions. With increasing particle concentration the jet had a tendency to leave the centreline position. With decreasing particle size, the suspensions showed a greater tendency to deviate from the centreline. The 0.5mm particle jet did not allow measurements exceeding 2.5%vol due to strong deviation from the centred position.

In future work it would be of interest to investigate particle flows by means of numerical methods. Large eddy simulations (LES) can capture large-scale fluctuations and periodic instabilities. To numerically identify the influence of particles, further detailed studies of multi-phase models must be conducted. If the effect of differences in particle size and concentration can be captured with computational fluid dynamics (CFD) should be investigated. A focus on MI phenomena and large-scale fluctuations would demand instationary calculations, where larger vortices are calculated directly rather than modelled (LES). It would be of great use for predictions of mixing and general particle flow, if numerical investigations could deliver improved capabilities for modelling particle properties and their effect on fluid flow.

Bibliography

[1] C. T. Crowe, M. Sommerfeld, Y. Tsuji, Multiphase flows with droplets and particles, CRC Press Inc, 1997.

[2] R. A. Gore, C. T. Crowe, International Journal of Multiphase Flow 15 (1989) 279–285.

[3] J.-i. Choi, O. Kwon, C. Lee, Journal of Physics: Conference Series 318 (2011) 052012.

[4] P. Hasal, J. Montes, H. Boisson, I. Fort, Chemical Engineering Science 55 (2000) 391–401.

[5] K. Bittorf, S. Kresta, Chemical Engineering Research and Design 81 (2003) 568–577.

[6] W. Bujalski, K. Takenaka, S. Paolini, M. Jahoda, A. Paglianti, K. Takahashi, A. Nienow, A. Etchells, Trans. IChemE (1999) 241 – 247.

[7] T. Zwietering, Chemical Engineering Science 9 (1958) 244–253.

[8] J. Kilander, F. Svensson, A. Rasmuson, AIChE journal 52 (2006) 4039–4051.

[9] M. Yianneskis, Z. Popiolek, J. Whitelaw, Journal of Fluid Mechanics 175 (1987) 537–555.

[10] D. Chapple, Chemical engineering science 49 (1994) 3651–3660.

[11] C. Galletti, a. Paglianti, K. C. Lee, M. Yianneskis, AIChE Journal 50 (2004) 2050–2063.

[12] M. Jahoda, V. Machon, L. Vlach, I. Fort, Acta Polytechnica (2002) 3–7.

[13] A. Paglianti, G. Montante, F. Magelli, AIChE Journal 52 (2006) 426–437.

[14] A. A. Townsend, Journal of the Franklin Institute 262 (1956) 517.

[15] J. Hinze, Turbulence, Mcgraw-Hill College, 1975.

[16] I. Wygnanski, H. Fiedler, Journal of Fluid Mechanics 38 (1969) 577–612.

[17] G. Batchelor, A. Gill, Journal of Fluid Mechanics 14 (1962) 529–551.

[18] J. Fan, H. Zhao, K. Cen, Experiments in Fluids 287 (1992) 279–287.

[19] H. Sheen, B. Jou, Y. Lee, Experimental Thermal and Fluid Science (1994) 315–327.

[20] Y. Hardalupas, A. Taylor, J. Whitelaw, Proceedings of the Royal Society of London. A. Mathematical and Physical Sciences 426 (1989) 31–78.

[21] R. N. Parthasarathy, in: ASME/JSME Fluids Engineering and Laser Anemometry Conference and Exhibition, volume 228, pp. 427 – 433.

[22] T. Virdung, a. Rasmuson, Chemical Engineering Science 62 (2007) 5963–5978.

[23] F. Durst, A. Melling, J. H. Whitelaw, Principles and Practice of Laser-Doppler Anemometry, Academic Press, 1981.

[24] N. R. Lomb 39 (1976).

[25] W. H. Press, S. A. Teukolsky, W. T. Vetterling, B. P. Flannery, Numerical Recipes in C, volume 29, Cambridge University Press, 1992.

[26] G. I. Taylor, Proceedings of the Royal Society of London Series A Mathematical and Physical Sciences 164 (1938) 476–490.

[27] S. Benayad, A. Salem, J. Legrand, Journal of Applied electrochemistry 30 (2000) 209–216.